



Multi-pass-cell-based nonlinear pulse compression to 115 fs at 7.5 μ J pulse energy and 300 W average power

JOHANNES WEITENBERG,^{1,2,*} ANDREAS VERNALEKEN,¹ JAN SCHULTE,² AKIRA OZAWA,¹ THOMAS SARTORIUS,² VLADIMIR PERVAK,¹ HANS-DIETER HOFFMANN,² THOMAS UDEM,¹ PETER RUSSBÜLDT,² AND THEODOR W. HÄNSCH¹

¹Max-Planck-Institut für Quantenoptik MPQ, Hans-Kopfermann-Str. 1, 85748 Garching, Germany

²Fraunhofer-Institut für Lasertechnik ILT, Steinbachstr. 15, 52074 Aachen, Germany

*johannes.weitenberg@mpq.mpg.de

Abstract: We demonstrate nonlinear pulse compression by multi-pass cell spectral broadening (MPCSB) from 860 fs to 115 fs with compressed pulse energy of 7.5 μ J, average power of 300 W and close to diffraction-limited beam quality. The transmission of the compression unit is >90%. The results show that this recently introduced compression scheme for peak powers above the threshold for catastrophic self-focusing can be scaled to smaller pulse energies and can achieve a larger compression factor than previously reported. Good homogeneity of the spectral broadening across the beam profile is verified, which distinguishes MPCSB among other bulk compression schemes.

© 2017 Optical Society of America

OCIS codes: (140.7090) Ultrafast lasers; (190.7110) Ultrafast nonlinear optics; (320.5520) Pulse compression; (320.7110) Ultrafast nonlinear optics.

References and links

1. P. Russbueldt, T. Mans, J. Weitenberg, H.-D. Hoffmann, and R. Poprawe, "Compact diode-pumped 1.1 kW Yb:YAG Innoslab femtosecond amplifier," *Opt. Lett.* **35**(24), 4169–4171 (2010).
2. R. Rußbüldt, H.-D. Hoffmann, M. Höfer, J. Löhring, J. Luttmann, A. Meissner, J. Weitenberg, M. Traub, Th. Sartorius, D. Esser, R. Wester, P. Loosen, and R. Poprawe, "Innoslab amplifiers," *IEEE J. Sel. Top. Quantum Electron.* **21**, 3100117 (2015).
3. C. J. Saraceno, F. Emaury, C. Schriber, A. Diebold, M. Hoffmann, M. Golling, T. Südmeyer, and U. Keller, "Towards millijoule-level high-power ultrafast thin-disk oscillators," *IEEE J. Sel. Top. Quantum Electron.* **21**(1), 1100318 (2015).
4. M. Müller, M. Kienel, A. Klenke, T. Gottschall, E. Shestaev, M. Plötner, J. Limpert, and A. Tünnermann, "1 kW 1 mJ eight-channel ultrafast fiber laser," *Opt. Lett.* **41**(15), 3439–3442 (2016).
5. C. Jocher, T. Eidam, S. Hädrich, J. Limpert, and A. Tünnermann, "Sub 25 fs pulses from solid-core nonlinear compression stage at 250 W of average power," *Opt. Lett.* **37**(21), 4407–4409 (2012).
6. S. Hädrich, M. Kienel, M. Müller, A. Klenke, J. Rothhardt, R. Klas, T. Gottschall, T. Eidam, A. Drozdy, P. Jójárt, Z. Várallyay, E. Cormier, K. Osvey, A. Tünnermann, and J. Limpert, "Energetic sub-2-cycle laser with 216 W average power," *Opt. Lett.* **41**(18), 4332–4335 (2016).
7. F. Guichard, Y. Zaouter, M. Hanna, F. Morin, C. Hönniger, E. Mottay, F. Druon, and P. Georges, "Energy scaling of a nonlinear compression setup using passive coherent combining," *Opt. Lett.* **38**(21), 4437–4440 (2013).
8. J. C. Travers, W. Chang, J. Nold, N. Y. Joly, and Ph. St. J. Russell, "Ultrafast nonlinear optics in gas-filled hollow-core photonic crystal fibers," *J. Opt. Soc. Am. B* **28**, A11–A26 (2011).
9. S. Hädrich, M. Krebs, A. Hoffmann, A. Klenke, J. Rothhardt, J. Limpert, and A. Tünnermann, "Exploring new avenues in high repetition rate table-top coherent extreme ultraviolet sources," *Light Sci. Appl.* **4**(8), e320 (2015).
10. M. Seidel, G. Arisholm, J. Brons, V. Pervak, and O. Pronin, "All solid-state spectral broadening: an average and peak power scalable method for compression of ultrashort pulses," *Opt. Express* **24**(9), 9412–9428 (2016).
11. M. Seidel, J. Brons, G. Arisholm, K. Fritsch, V. Pervak, and O. Pronin, "Efficient high-power ultrashort pulse compression in self-defocusing bulk media," *Sci. Rep.* **7**(1), 1410 (2017).
12. M. Bache, O. Bang, W. Krolikowski, J. Moses, and F. W. Wise, "Limits to compression with cascaded quadratic soliton compressors," *Opt. Express* **16**(5), 3273–3287 (2008).

13. Y. C. Cheng, C.-H. Lu, Y.-Y. Lin, and A. H. Kung, "Supercontinuum generation in a multi-plate medium," *Opt. Express* **24**(7), 7224–7231 (2016).
14. J. Schulte, T. Sartorius, J. Weitenberg, A. Vernaleken, and P. Russbuedt, "Nonlinear pulse compression in a multi-pass cell," *Opt. Lett.* **41**(19), 4511–4514 (2016).
15. M. Hanna, X. Délen, L. Lavenu, F. Guichard, Y. Zaouter, F. Druon, and P. Georges, "Nonlinear temporal compression in multipass cells: theory," *J. Opt. Soc. Am. B* **34**(7), 1340–1347 (2017).
16. M. Herrmann, M. Haas, U. D. Jentschura, F. Kottmann, D. Leibfried, G. Saathoff, Ch. Gohle, A. Ozawa, V. Batteiger, S. Knünz, N. Kolachevsky, H. A. Schüssler, Th. W. Hänsch, and Th. Udem, "Feasibility of coherent xuv spectroscopy on the 1s-2s transition in singly ionized helium," *Phys. Rev. A* **79**(5), 052505 (2009).
17. S. Hädrich, J. Rothhardt, M. Krebs, F. Tavella, A. Willner, J. Limpert, and A. Tünnermann, "Single-pass high harmonic generation at high repetition rate and photon flux," *J. Phys. At. Mol. Opt. Phys.* **49**(17), 172002 (2016).

1. Introduction

Ultrafast lasers have manifold scientific and industrial applications, relying on the short pulse duration, high peak power or temporal coherence they provide. Many applications benefit from short pulse duration and high average power, which however are difficult to achieve simultaneously. While laser systems based on Ti:sapphire easily reach pulse durations <100 fs, they are typically limited to few W in average power. Yb-based laser systems on the contrary reach many 100 W of average power [1–5], but are limited to pulse durations of several 100 fs at that power level due to the gain bandwidth. External nonlinear pulse compression allows combining the high average power of Yb-based lasers with short pulse durations. The compression relies on nonlinear spectral broadening via self-phase modulation by the Kerr effect and subsequent chirp removal.

Established schemes for nonlinear spectral broadening are limited in the pulse energy range they can be applied to. Broadening in a dielectric waveguide is limited to pulses with peak powers below the material's critical power for self-focusing due to the Kerr effect, which is 4 MW for fused silica and linearly polarized light, corresponding to 3 μ J pulse energy at 800 fs. Note that it is the peak power that is limited due to catastrophic self-focusing; increasing the cross section to reduce intensity does not help. The highest average power for compression with a dielectric nonlinear medium has been achieved by broadening in a photonic-crystal fiber, yielding compressed pulses with 250 W, 23 fs pulse duration and 1 μ J pulse energy [5].

For higher pulse energies, spectral broadening in capillaries filled with a noble gas is usually applied. Due to the smaller nonlinearity of gases compared to dielectrics, the critical power is accordingly larger and catastrophic self-focusing can be avoided by choosing a suitable gas and pressure. The highest average power achieved with this scheme is 408 W with 30 fs and 320 μ J pulse energy [6]. Due to the small nonlinearity of gases and limitations in length and diameter of the capillaries (related to loss and practicality), this scheme is limited to pulse energies >100 μ J.

Much effort has been made over the last years to bridge the gap of pulse energies in the range of 3–100 μ J that is not covered by these schemes. Higher pulse energies in dielectric waveguides are possible by divided-pulse compression, i.e. splitting the pulses into several replicas which are recombined after propagation through the nonlinear medium. Compressed pulses with 7.5 μ J pulse energy, 71 fs and 0.75 W have been achieved [7]. However, power scalability is yet to be demonstrated. Using gas-filled hollow-core fibers instead of capillaries allows broadening pulses well below 100 μ J because they have smaller diameters and can be longer without considerable loss [8]. The highest compressed average power achieved is 76 W with 7 μ J pulse energy and 31 fs pulse duration [9]. Hollow-core fibers hold promise to allow pulse compression at even higher average power. Ionization of the gas might have to be considered as a limitation.

A different approach is to omit the waveguide and achieve spectral broadening at free propagation through a bulk dielectric [10–13]. This allows using peak powers well above the critical power for self-focusing, accessing the energy range 3–100 μ J. Indeed, the peak power

has to be above the critical power, in order to acquire a considerable nonlinear phase and spectral broadening at free propagation, i.e. without a waveguide confining the beam with high intensity along the interaction length with the medium. Catastrophic self-focusing is avoided for a beam with precisely adjusted diameter and divergence and a suitable length of the nonlinear medium. A compressed average power of 30 W with 43 fs and 0.8 μJ pulse energy has recently been demonstrated [10]. Omitting the waveguide can be considered an advantage, because coupling a beam into a waveguide is challenging at high average power, which typically goes along with beam pointing fluctuations and a limited beam quality, which can destroy the waveguide. However, spectral broadening at a single pass through a bulk nonlinear medium is inevitably inhomogeneous across the beam profile, which necessitates subsequent spatial filtering, thereby inherently limiting the compression efficiency. The homogeneity is somewhat improved by using a medium with a negative nonlinear index of refraction [11,12].

We recently demonstrated a novel scheme, which avoids a waveguide and mitigates the disadvantages of nonlinear spectral broadening in a single bulk medium [14]. This makes it robust, power-scalable and efficient at the same time. The scheme relies on the repeated propagation through a nonlinear medium with only small nonlinear phase for each step and propagation without nonlinearity in-between. This can be achieved in a compact setup with a multi-pass cell (MPC), and can be called multi-pass cell spectral broadening (MPCSB). We demonstrated a compressed average power of 375 W, 170 fs pulse duration, 37.5 μJ pulse energy and an almost preserved beam quality factor $M^2 = 1.3$ [14].

In MPCSB nonlinear compression for pulses with peak powers above the critical power catastrophic self-focusing is avoided by choosing a small nonlinear phase per step. If these steps are suitably combined, i.e. with propagation without nonlinearity in-between, the Kerr lensing effect of the steps does not add up in a self-amplifying way, as would be the case for directly joining the steps: a stronger lensing in one step does not necessarily translate into a smaller beam at the next step, as can be seen by *ABCD*-matrix analysis. The MPC represents a periodic system with a distinguished *q*-parameter, which is reproduced at propagation from one mirror to the other. We call this the eigen-*q*-parameter of the MPC. The Kerr lensing can be modelled as an additional focusing element in the MPC (or periodic optical system in general), which changes its eigen-*q*-parameter. The eigen-*q*-parameter will therefore be a function of the instantaneous power. The MPC is designed to yield a small change of the eigen-*q*-parameter for the instantaneous powers within the temporal pulse profile. This ensures homogeneous spectral broadening, because it corresponds to a small change of the *q*-parameter across the spectrum for the chirped pulse after spectral broadening (which is equivalent to a small change of the spectrum across the beam profile). This change can be quantified by the spatial overlap between the eigen-*q*-parameter for the peak power and for vanishing power, which is determined by the nonlinear phase per step and by the position in the stability range of the MPC. The demand of an overlap close to unity restricts the nonlinear phase per step to values much smaller than π . Values up to $\pi/10$ seem reasonable for a MPC with a suitable position in the stability range. The effectiveness of the MPCSB approach in mitigating spatially inhomogeneous broadening has recently been studied and verified by numerical simulation [15]. Nonlinear spectral broadening setups with multiple nonlinear steps have been suggested and demonstrated before [10,13], however with much larger nonlinear phase per step and without considering the spatial homogeneity of the broadening.

The purpose of this paper is twofold. Firstly, we report on the implementation of the MPCSB compression scheme with smaller pulse energy and larger compression factor than for the previous demonstration, demonstrating the suitability of the scheme for these parameters. Secondly, we verify homogeneous spectral broadening by measuring the spectrum spatially resolved across the beam profile and the beam quality and beam parameters spectrally resolved across the spectrum.

The objective of the reported laser system is a frequency comb in the extreme ultra-violet (EUV) in order to perform high-precision spectroscopy of the 1s-2s transition in helium⁺ ions [16]. An EUV comb at 60.8 nm wavelength to drive this 2-photon transition can be achieved by high-harmonic generation (HHG) of an infrared comb around 1033 nm (using the 17th harmonic). In order to achieve sufficient EUV power, high average power and short pulse duration of the infrared system are needed. High average power is essential to reach large pulse energy for the highly nonlinear HHG process at the high repetition rate dictated by the frequency comb. Additionally, an enhancement resonator can be employed, which yields an increased power for resonator-enhanced HHG. Short pulse duration is important in order to achieve an acceptable conversion efficiency, which is impacted by ionization of the noble gas serving as the HHG nonlinear medium.

A 400 W Yb:YAG Innoslab amplifier [2] is available for the spectroscopy setup. The bandwidth of the amplified pulses is 2 nm, allowing pulse durations around 700 fs, which is too long for efficient HHG [17]. Besides, the spectrum is centered at 1030 nm and does not cover the required wavelength. External pulse compression by nonlinear spectral broadening is therefore indispensable. The repetition rate is chosen to 40 MHz as a trade-off between large pulse energy (on the order of 10 μ J) and manageable length of the enhancement resonator. The MPCSB scheme is the only reported scheme proven capable of compressing pulses with this intermediate energy at this average power level. The setup is adapted to the higher repetition rate and smaller pulse energy compared to the experiments in [14] by using a nonlinear element in the middle of the MPC, where the beam cross section is smaller, instead of using the substrates of the MPC mirrors as the nonlinear elements. In terms of the suppression of the Kerr lens action these two MPC geometries are equivalent. In order to avoid catastrophic self-focusing and to achieve a small change of the eigen- q -parameter with the instantaneous power, it is essential to have propagation between the nonlinear steps. It does not matter, if the nonlinear element is at the beam waist or at a convergent/divergent beam. The number of passes through the nonlinear element is increased from 38 to 57 in order to achieve a larger nonlinear phase and compression factor.

2. Experimental setup

The setup comprises the following elements [see Fig. 1]. The seed laser is a commercial comb-ready fiber-laser system (femto orange, Menlo Systems) which is customized for 40 MHz repetition rate and a spectral width of 3.0 nm (FWHM) in order to match the Innoslab amplifier's gain bandwidth. It reaches 4.3 W at full pump current and is operated with 3.0 W output power. The beam quality factor is $M^2 = 1.12 \times 1.06$. It seeds a high-power Yb:YAG Innoslab amplifier as described in [2]. The amplifier contains a slab-shaped high-power isolator and a cylindrical telescope to shape a round output beam. It reaches an output power of 370 W (400 W before isolator). The beam quality factor is $M_x^2 \times M_y^2 = 1.08 \times 1.42$, where y denotes the slow-axis of the slab crystal [2]. The bandwidth is reduced to 2.0 nm (FWHM) by gain narrowing. The pulse duration is 860 fs (FWHM), which is larger than bandwidth-limited (factor ~ 1.2). This stems from the spectral phase of the seed laser, which is also not bandwidth-limited with 700 fs pulse duration at 3.0 nm bandwidth. Measuring the seed laser's spectral phase at various pump currents confirms that this is due to nonlinear effects in the main amplifier gain fiber of the seed laser system. Nonlinearity in the Innoslab amplifier on the contrary is negligible [1], although it amplifies unchirped pulses, i.e. does not employ chirped-pulse amplification (CPA). A spatial filtering module improves the beam quality of the amplified beam to $M_x^2 \times M_y^2 = 1.07 \times 1.20$ by removing 10% of the power, filtering the profile in y -direction with a slit mirror. The setup also includes a 4-dimensional beam-pointing stabilization and a variable attenuator consisting of a motorized wave-plate and a thin-film polarizer.

The MPC for nonlinear spectral broadening consists of two concave-convex mirrors with 50.8 mm diameter and 300 mm radius of curvature. The concave surface oriented towards the

center of the MPC is coated with a dispersive HR coating with $GDD = -(250 \pm 50) \text{ fs}^2$ in order to compensate for material dispersion in the nonlinear element. The convex back sides are AR-coated. The ray bundle leaking through one of the mirrors is focused to a CCD camera using two achromatic lenses with 50 mm diameter. Two AR-coated fused-silica plates with 25 mm diameter and 12 mm thickness are placed in the middle of the MPC to serve as nonlinear elements. A single thicker element would be equivalent but was not available. Coupling to and from the cell is achieved with scraper mirrors of 5 mm width.

The MPC and the input beam are aligned to form a circle of 29 evenly spaced reflections on each mirror (one of which is screened by the scraper) with the beam advancing by 5 position along this circle each time it hits the mirror. This yields 57 passes through the nonlinear elements. The beam diameter for a Gaussian beam with eigen- q -parameter of the MPC is $2w_1 = 1.19 \text{ mm}$ and $2w_0 = 0.32 \text{ mm}$ on the mirrors and in the middle of the MPC; a Kerr lens corresponding to a nonlinear phase of 0.07π changes the diameters to 1.07 mm and 0.35 mm, respectively. The total distance propagated in glass and in air is 1.37 m and 30.8 m, respectively.

Mode-matching, i.e. adaption of the input beam's q -parameter to the eigen- q -parameter of the MPC, is achieved with a single spherical lens. Similarly, the output beam is collimated with a single spherical lens. The CCD camera allows evaluating the mode-matching, which yields beam diameters varying by $\pm 10\%$ along the circle of spots.

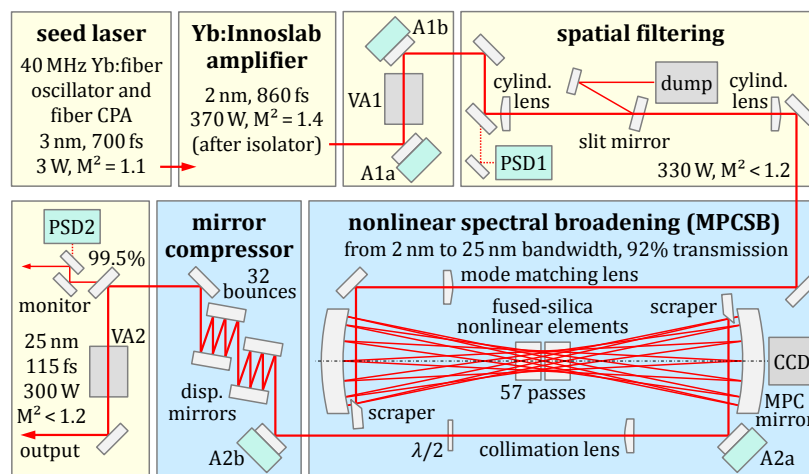


Fig. 1. Sketch of the setup for nonlinear pulse compression. The blue boxes contain the compression unit. VA1, VA2 – variable attenuators; A1a, A1b, A2a, A2b – actuators for beam pointing stabilization; PSD1, PSD2 – position-sensitive detectors; CCD – camera for evaluation of mode-matching.

The spectrally broadened pulses are sent through a mirror compressor with a total GDD of $-34,000 \text{ fs}^2$ (32 reflections distributed on 12 mirrors with GDD of $-1,000 \text{ fs}^2$ and $-1,300 \text{ fs}^2$). Another 4-dimensional beam pointing stabilization is included with both actuators after the MPC and the position sensor after the compressor. This stabilization is necessary, because the MPC and the compressor add pointing fluctuations. We attribute this to moving air heated by hot mirror surfaces. The temperature increase of the MPC mirrors and compressor mirrors at full power is estimated to $\sim 20 \text{ K}$ ($\sim 3 \text{ K}$ more at the position of the reflections) for all mirrors by inspection with a thermal camera. The mounts and apertures of the MPC and compressor are water-cooled and they are placed inside a non-sealed housing. The housing reduces air movement driven by the flow modules above the optical table. The beam pointing fluctuation is similarly reduced, when the flow modules are switched off with opened lid of the housing. Due to the small additional temperature increase at the position of the reflections we estimate thermal lensing in the mirrors to be weak. Another variable attenuator is installed behind the

mirror compressor. A turning mirror in front of the attenuator transmits 0.5% of the power as a monitor output.

3. Nonlinear compression results

The power at the second variable attenuator is 303 W, corresponding to a transmission of the compression unit of 91%. This transmission is independent of the power sent to the MPC; it is therefore dominated by linear losses. Transmission measurements at small power assign a transmission of 92.0% for the MPC and 99.3% for the mirror compressor. The pass through the MPC contains 58 reflections on the MPC mirrors (>99.95% manufacturer specification) and 228 passes through the AR coating of the nonlinear elements (<0.05% manufacturer specification), furthermore 4 turning mirrors, 2 lenses and a wave-plate. The residual reflectivity of the nonlinear elements must be well below the specifications, which agrees with an independent measurement yielding ~50 ppm. Some loss stems from slight clipping at the scraper mirrors.

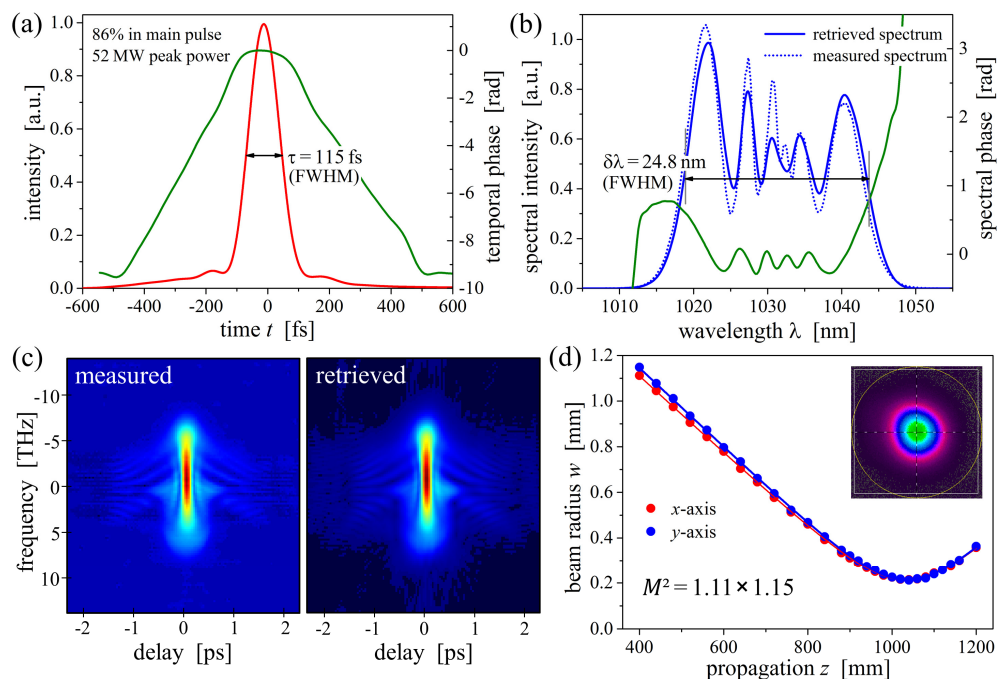


Fig. 2. Experimental results of compressed pulses at 300 W average power and 7.5 μJ pulse energy. (a) Temporal pulse shape and phase retrieved from FROG measurement, (b) spectrum and spectral phase retrieved from FROG measurement and spectrum measured with optical spectrum analyzer, (c) FROG traces (left measured, right retrieved), (d) beam quality measurement and profile at the beam waist.

Spectral broadening to 24.8 nm (taken at half the intensity of the outer spectral maxima) and a compressed pulse duration of 115 fs (FWHM) is achieved at full power. The Fourier-transform limit of the spectrum is 99 fs (FWHM). A fraction of 86% in the main pulse and a peak power of 52 MW are inferred from the frequency-resolved optical gating (FROG) measurement. This corresponds to spectral broadening by a factor of 12, pulse shortening by a factor of 7.5, and peak power increase by a factor of 6. The beam quality is preserved by the compression unit with $M^2 = 1.11 \times 1.15$ for the compressed pulses. Results of the measurements with FROG, optical spectrum analyzer and M^2 meter are shown in Fig. 2.

The dispersive coating of the MPC mirrors only partly compensates the material dispersion ($GDD = 450 \text{ fs}^2$ for 2x 12 mm with $19 \text{ fs}^2/\text{mm}$), leaving a GDD of 200 fs^2 for every prop-

agation between the MPC mirrors and $12,000 \text{ fs}^2$ for a complete pass through the MPC. This results in a measured pulse duration of 1.67 ps (FWHM) after the MPC and explains the incomplete modulation of the broadened spectrum (the spectral intensity not reaching zero between the maxima in the spectrum) and the large amount of GDD needed for the compressor. The setup was originally planned with a single nonlinear element of thickness 13 mm and compensated GDD . This did however not yield sufficient spectral broadening.

Because of the increasing pulse duration in the MPC, the nonlinear phase per pass through the nonlinear elements decreases; we estimate an average nonlinear phase of 0.07π per pass and an accumulated nonlinear phase of 4π after a complete pass through the MPC. This estimate is derived from the beam diameter in the middle of the cell including the M^2 factor and an average peak power of $\sim 6.5 \text{ MW}$.

4. Homogeneity of spectral broadening

In general, nonlinear spectral broadening by free-space propagation through the nonlinear medium is expected to be inhomogeneous across the beam profile. This is however avoided for MPCSB by restricting each pass through the nonlinear medium to a small nonlinear phase and suitably combining these steps with free-space propagation in-between. Inhomogeneous broadening, i.e. a varying spectral width across the profile, would also mean different q -parameters across the spectrum, which would result in a reduced beam quality. Therefore, the preserved M^2 value already indicates reasonable homogeneity.

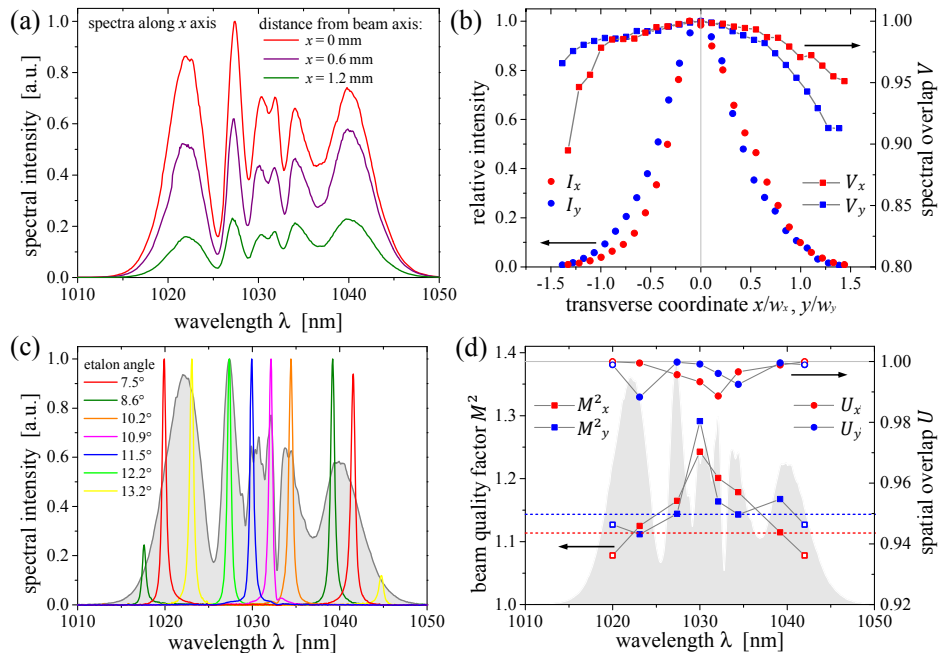


Fig. 3. Characterization of the homogeneity of the spectral broadening. (a) Spectra across the beam profile, (b) relative intensity and spectral overlap V across the beam profile along both transverse axes, (c) unfiltered spectrum and filtered spectra for spectrally resolved beam quality measurement (measured with fiber-coupled spectrometer), normalized to unity maximal spectral intensity (d) beam quality factor M^2 and spatial overlap U across the spectrum. The dashed lines indicate the beam quality factor of the unfiltered beam. The open symbols correspond to the measurement with spectral components on both sides of the spectrum, which cannot be assigned to a single wavelength.

We characterize the homogeneity of the spectral broadening by measuring the spectrum across the transverse profile of the compressed beam, collimated to a beam diameter of $2w_x \times 2w_y = 2.7 \text{ mm} \times 2.8 \text{ mm}$. A multimode fiber ($400 \mu\text{m}$ core diameter) with FC/PC tip is

scanned across the profile in steps of 0.15 mm along both transverse axes and spectra are recorded with an optical spectrum analyzer [Fig. 3(a)]. The overlap of each spectrum $I(\lambda)$ with the spectrum on the beam axis $I_0(\lambda)$ is calculated as $V = \frac{[\int I(\lambda) \cdot I_0(\lambda)]^2 d\lambda}{[\int I(\lambda) d\lambda] \cdot [\int I_0(\lambda) d\lambda]}$, and plotted vs. transverse coordinate in Fig. 3(b). The overlap drops at the edge of the beam profile but is $V > 89\%$ for all recorded spectra. By weighting the overlap with the intensity an effective overlap of $V_x = 99.5\%$ and $V_y = 99.2\%$ is calculated.

The relative weight of the spectral lobes at the short and long wavelength side changes across the beam profile in x -direction, i.e. the centroid of the spatially resolved spectra changes [Fig. 3(a)]. While a small change of the spectral width across the beam profile is expected due to inhomogeneous self-phase modulation at each nonlinear step, the shift of the centroid would not be expected for a symmetric beam profile and homogeneous start beam. We attribute this to an inhomogeneity of the start beam, which probably stems from the CPA compressor in the seed laser system. The centroid of the seed spectrum shifts by 0.75 nm across the beam diameter ($1/e^2$ intensity) along the x -direction (in which the beam is dispersed in the compressor).

Additionally we perform spectrally resolved beam-quality measurements by filtering the beam spectrally with an etalon of free spectral range 22 nm, finesse 45 and free aperture 20 mm, tilted to select different wavelengths. The free spectral range of the etalon is smaller than the spectral width of the broadened spectrum. Therefore, as the incidence angle is tuned, the etalon eventually samples two different spectral regions of the broadened spectrum; one measurement is performed for an incidence angle of 7.5° , where the two filtered spectral regions contribute equally to the filtered spectrum [Fig. 3(c)]. The simultaneous sampling of two spectral regions could have been avoided by using a dielectric bandpass filter with similar bandwidth (0.5 nm) instead of the etalon, which however was not available for the experiment. A spherical telescope in front of the etalon is used to expand the beam to a diameter of 3.6 mm and collimate it to a divergence half angle of 0.2 mrad. The beam quality factor M^2 clearly differs across the spectrum. It is smallest for the outer spectral lobes and largest at the center. This might be expected, because the outer spectral lobes originate from the part of the pulse with the largest temporal intensity slope, which does not coincide with the highest intensity and strongest Kerr lens, while the other spectral components are superpositions from different parts of the pulse with different Kerr lens strength. The spatial overlap with the unfiltered beam is calculated for each spectral component from the q -parameter $q = z_q + iz_R$ obtained from the hyperbolic fit to the beam caustic as $U = 4(z_R \cdot z_{R0}) / [(z_R + z_{R0})^2 + (z_q - z_{q0})^2]$, where $q_0 = z_{q0} + iz_{R0}$ is the q -parameter of the unfiltered beam. This equation follows from the evaluation of the overlap integral $U = \frac{|\int E(r) \cdot E_0^*(r) 2\pi r dr|^2}{[\int |E(r)|^2 2\pi r dr] \cdot [\int |E_0(r)|^2 2\pi r dr]}$ between two Gaussian beams given by the electric fields $E(r)$ and $E_0(r)$ and the q -parameters $q = z_q + iz_R$ and $q_0 = z_{q0} + iz_{R0}$, respectively. It is therefore only valid for Gaussian beams. Here the equation is used as a measure of how strong the q -parameter varies across the spectrum. An evaluation of the spatial overlap including the (spectrally varying) beam quality would only be possible, if the electric fields were known; it cannot be evaluated from the measured beam quality factors alone. The so defined spatial overlap is $U > 98.5\%$ for all measured wavelengths [Fig. 3(d)]. All beam diameters differ less than 17.5% and 14% from the unfiltered beam in x - and y -direction, respectively. The spatial overlap and variation in beam diameter matches the strength of the Kerr lens corresponding to a nonlinear phase of 0.07π , which yields a maximal change of the beam diameter corresponding to the eigen- q -parameter of 11%, i.e. an overlap of 98.9% between the eigen- q -parameters with and without Kerr lens.

5. Scope of the MPCSB compression scheme

The MPCSB pulse compression scheme has a number of attractive properties. Because it avoids a waveguide or restricting apertures, it is insensitive to fluctuations of the beam point-

ing or profile and can be applied to imperfect beam quality [14]. The scheme can be very efficient, because loss at coupling to a waveguide is avoided, and the transmission is determined only by the reflectivities of the HR and AR coatings. These properties make it especially suitable for high average power.

The scheme can be applied to a large range of pulse energies and pulse durations. The intensity in the nonlinear element has to be chosen to stay well below the damage threshold. It should not be chosen too small, however, because this would need a longer element to reach a nonlinear phase on the order of $\pi/10$ with a larger material dispersion to be compensated by the dispersive MPC mirrors. For smaller pulse energies the nonlinear element can be placed in the middle of an MPC with a small beam size (as in this setup). In order to reach the nonlinear phase with a thickness of the element which is smaller than the Rayleigh length, the peak power should be well above the critical power. This corresponds to several μJ at 800 fs pulse duration and fused silica. For somewhat smaller pulse energies a material with smaller critical power can be employed. For larger pulse energies the MPC mirrors can be used as nonlinear elements (as in the first demonstration [14]), where the larger beam size matches the larger pulse energy. The upper limit of the pulse energy is given by the damage threshold together with a limitation in beam size, which depends on the MPC length and the position in the stability range. For a length of $L \leq 1$ m and not too close to the stability edge (e.g. $L/(2R) \leq 99\%$, with radius of curvature R), a beam cross section of 0.05 cm^2 (at $1 \mu\text{m}$ wavelength) is possible. With a fluence of e.g. 20 mJ/cm^2 this corresponds to a pulse energy of 0.5 mJ .

The scheme can be used for starting pulse durations in the ps and fs range. The limitation towards short pulses is given by the bandwidth of the MPC optics, which need to provide small loss at HR and AR surfaces and dispersion compensation across the bandwidth of the spectrally broadened pulses. For a bandwidth of e.g. 200 nm around 1030 nm a compressed pulse duration below 20 fs should be feasible. The compression factor is determined by the accumulated nonlinear phase, i.e. by the number of steps and the nonlinear phase per step. The nonlinear phase per step determines the variation of the eigen- q -parameter across the temporal pulse profile, and should be limited to values $\lesssim \pi/10$ for good homogeneity. A larger number of passes requires large optics and increases loss. We expect that a somewhat larger compression factor than demonstrated here (factor 7.5) can be achieved with a single compression stage by increasing the nonlinear phase for each step. For larger compression factors two (or more) compression stages can be applied.

A possible disadvantage of the MPCSB compression scheme is the very long propagation distance (32 m in this setup). This can lead to pointing fluctuations and introduces a delay which e.g. limits the bandwidth for a phase-stabilization setup, with a detector behind the pulse compression and giving feedback to the laser to pre-compensate the noise.

6. Summary

To conclude, we have demonstrated pulse compression from 860 fs to 115 fs at 300 W average power, $7.5 \mu\text{J}$ pulse energy and close to diffraction-limited beam quality by means of nonlinear spectral broadening in a multi-pass cell (MPCSB). The compression efficiency is $>90\%$. We have verified good homogeneity of the spectral broadening by a spatially resolved measurement of the spectrum as well as a spectrally resolved measurement of q -parameter and beam quality.

Funding

Deutsche Forschungsgemeinschaft (DFG) (Cluster of Excellence 158, Munich-Centre for Advanced Photonics, MAP); Max-Planck Fraunhofer cooperation project KORONA; European Union's Horizon 2020 research and innovation programme (664732, nuClock).